Semi-Packed Gas Chromatography Columns With Density Modulated Pillars

Ryan Chan and Masoud Agah

***Abstract*— The separation column is the most important component which influences the performance of gas chromatography systems. Among a number of column designs, the microfabricated semi-packed column has attracted particular attention in micro gas chromatography because it enhances the separation efficiency and provides higher sample capacity compared to the open-channel counterparts. However, these added advantages come at the cost of higher pressure drops per unit length of the separation column. This paper reports new semi-packed column designs through density modulation of the pillars by changing the spacing between rows or the number of pillars per row from. Various geometries were fabricated and tested against regular semi-packed columns having either one pillar or four pillars per row. Different performance metrics were measured including column pressure drop, optimal flow velocity, number of theoretical plates, and separation efficiency. The density-modulated semi-packed columns provide efficiencies comparable with that of semi-packed columns embedding more pillars per row while requiring a lower inlet pressure which is more comparable with the columns embedding one pillar per row. These density-modulated columns were able to successfully separate diesel and kerosene compounds and to identify the major hydrocarbon constituents of these two widely used samples. [2018-0102]**

***Index Terms*— Density modulation, MEMS, micro gas chromatography, micro pillars, semi-packed, separation column.**

I. Introduction

GCHROMATOGRAPHY (GC) is used in a variety of fields where the monitoring of volatile organic compounds (VOCs) is of importance [1]. Standard GC tools and systems are bulky and consume high power during operation. The current trend in this field is moving towards miniaturizing the system to allow for field and point-of-care usage. Microsystems-based GCs allow for great portability, reduced sampling and analysis times, and lower power consumptions [2]–[11].

The heart of a GC is the column which is responsible for the separation of different components of a mixture before detection. The separation is due to differential interaction of the components of a mixture with the stationary phase coating of the column. As the compounds of the mixture flow through the separation column, they spend the same time in the inert carrier gas that pushes the sample through the column. However, they adsorb or desorb at different rates depending on their affinity to the stationary phase. This affects the time that spend by each compound in the stationary phase and hence affecting the overall time required for each compound to pass through the entire column. The compounds separated in time and space are then detected at the outlet of the column as they pass over a detector and their chromatographic response can be recorded. In most GCs, the separation column is an open tubular fused silica capillary tubing having a stationary phase on its inner wall. Changing the length of the column or the stationary phase coating will subsequently change the behavior of the column and the GC separation performance including the resolution, peak shape and capacity, and separation selectivity.

The development of planar columns fabricated using microelectromechanical systems (MEMS) technology is a solution for reducing the footprint of the separation component, for reducing cost through batch fabrication, for integrating heaters and temperature sensors for fast and complex analysis, and for decreasing overall size and power requirements. Different research groups are working to develop different geometries, topographies, and stationary phases in order to improve the chromatographic performance of MEMS columns [12]–[19]. Early work in this area were primarily focused on simple microfluidic channels etched in silicon and bonded to a Pyrex wafer [7], [20]–[22]. These column cross sections were determined based on the type of etch performed to create the channels defined by photolithography techniques. Depending on the etching method used, these channels had either rectangular or more circular cross sections [7], [23]. These early columns were typically coated with conventional stationary phases such as OV-1 to mimic a planar and miniaturized version of the open tubular columns used in conventional GCs [7], [20], [24].

In an attempt to improve the performance of these early micro columns (μCs), research was directed at changing the geometries and topographies of the micro-channels to improve upon different parameters. The multi-capillary μC design first introduced by our group was developed in order to improve upon the separation efficiency without sacrificing sample capacity [25]. This was based off of the Golay equation which indicates that reduction in sample capacity by decreasing the inner-diameter of a column can be compensated by increasing the number of parallel capillaries [26]. The work showed that

Manuscript received May 7, 2018; revised November 1, 2018; accepted November 10, 2018. Date of publication December 5, 2018; date of current version February 1, 2019. This work was supported by the National Science Foundation through ECCS under Grant 1711699. Subject Editor A. J. Ricco. *(Corresponding author: Ryan Chan.)*

The authors are with the Department of ECE, Virginia Tech, Blacksburg, VA 24061 USA (e-mail: ryanchan@vt.edu).

This paper has supplementary downloadable material available at http://ieeexplore.ieee.org, provided by the author.

Color versions of one or more of the figures in this paper are available online at http://ieeexplore.ieee.org.

Digital Object Identifier 10.1109/JMEMS.2018.2881532

a column consisting of four parallel channels 65μm wide provided a sample capacity twenty times that of a single 50μm wide channel. However, it also noted that conventional coating techniques failed to produce a high yield when multi-capillary columns with a large number of parallel capillaries were used.

Among different MEMS-enabled columns, the semi-packed columns (SPCs), also reported by our group, provide improved separation efficiency and sample capacity when compared to their open rectangular counterparts [27], [28]. In addition, it also helps to suppress the coating issues faced in multi-capillary configurations. By embedding pillars into the channel, the effective channel width is reduced and the internal surface area is increased. This allows for easier coating using established conventional coating techniques as there is a larger single volume compared to multiple smaller volumes. The increase in surface area also allows for more of the stationary phase coating thereby increasing the sample capacity. The embedded pillars also reduce the distance of mass transfer which helps create a more uniform interaction between the mobile and stationary phases. Similarly, the flow velocity profile is also more uniform after including the embedded pillars which can reduce band broadening [27], [29]. Work is constantly being conducted with the hope of optimizing this semi-packed design. For example, several groups have reported on the effect of the pillar shape to generate a more even flow velocity profile [29]. Pillar density is also something that has been used to tune the separation efficiency [30]–[33]. Research has even been conducted on the shape of the channels and how it can affect the GC performance [13], [14], [34]. However, while the SPC design has a lower pressure requirement than the multi-capillary columns, they still have a much higher requirement compared to an open rectangular μC. This problem is exacerbated further when pillar density is increased monotonically through the entire channel to further improve the separation efficiency [25], [30], [31].

Another μC design that has been reported by our group is the width-modulated column [12]. Compared to a standard open rectangular column, these width-modulated devices performed more favorably due to the change in the channel width over the length of the column. This is due to the separation efficiency being proportional to the square of the channel width. As the channel becomes smaller, the local separation efficiency increases which leads to the overall column becoming more efficient as a result [12]. Modulation of the column width or the thickness of stationary phase in a column is an old concept of GC dating back to 1962 where it is believed that diminishing the interaction between mobile and stationary phase could provide similar effects as temperature or pressure programming [35]. Following our previous work, this paper reports a new μC design based on the combination of two MEMS column topographies: SPC and width modulation. These designs demonstrate that instead of using a high density of pillars in an SPC, a modulation of the pillar density over the length of the column can result in high resolution separations of complex mixtures without requiring high pressures when compared to semi-packed columns having a high density of pillars. Even though the focus of this paper is the development of new MEMS GC columns, it is worth mentioning that the columns reported here are coated with a room-temperature ionic liquid. These stationary phases offer unique separation capabilities and their successful integration with MEMS columns have already been demonstrated [36].

TABLE I
DIFFERENT DENSITY MODULATED SEMI-PACKED COLUMN DESIGN VARIATIONS OF TOPOGRAPHY AND GEOMETRY

DMSPC Variation	Topography	Geometry
A	Row pitch spacing	Low to high
B	Row pitch spacing	Repeated
C	Pillars per row	Low to High
D	Pillars per row	Repeated

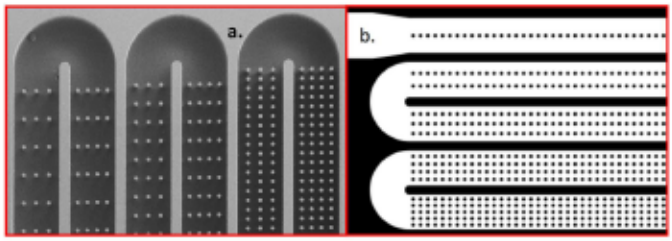

Fig. 1. (a) SEM of DMSPC using pillar row pitch distance to modulate density, (b) portion of mask showing DMSPC using number of pillars to modulate density.

II. COLUMN DESIGN AND FABRICATION

A. Design

Four distinct density modulated semi-packed columns (DMSPC) as indicated in Table 1 along with two regular semi-packed columns as control geometries were designed and fabricated in this work. These new DMSPCs relies upon the embedded micro-pillars to improve the separation efficiency over a standard open rectangular column but does so in a way that does not require the same pressure requirements of semi-packed columns with high density pillars. This density modulation was achieved by creating different modulation approaches for the embedded pillars. The length and width of the columns for all these cases were kept at 1 m and 190 μm, respectively. Design A and B in Table 1 are based on changing the row pitch between the embedded pillars. Figure 1a shows a top-down scanning electron microscopy (SEM) view of these scenarios. Specifically, the row pitch changes from 120μm at its least dense, to 80μm row pitch spacing, to 40μm at its most dense. Added to that, the number of pillars also alternates between three and four as seen in Figure 1a. The combination of row pitch and the number of pillars create six different topographies. In Design A, the entire column length is divided into 6 sections and each section has one of the above topographies. In Design B, every 10 cm of the column length has all those 6 topographies and then repeats itself.

The details of these designs can be found in supplementary documents. In both Design A and B, where the local volume is larger, there is less flow resistance due to reduced number of the embedded pillars. As the density of the embedded pillars increases, however, the local separation efficiency improves. Designs C and D take advantage of the concept of "virtual walls" in semi-packed columns [33]. These virtual walls are dependent on the row pitch spacing. In these designs, a row pitch of 40μm was maintained through the column length but modulation achieved by varying the number of pillars per row from one to five as seen in Figure 1b. Design C mirrors the width modulation in that the density of the embedded pillars is lowest at the inlet and transitions to the highest density over the length of the column. Each 20 cm of the column length has the same number of pillars per row. Design D follows the repeated topography. More specifically, the first 10cm of the column length is divided into 5 equal sections where each section has a specific number of pillars per row. This pattern repeats itself through the length of the column. The details of Design C and D can also be found in the supplementary documents.

B. Fabrication

The fabrication process for these devices is similar to previously reported columns [3], [37]. Silicon wafers (100 orientation, n-type, 4 inch diameter, 500μm thickness, single side polished, purchased from UniversityWafer, 11 Elkins Street, Unit 330, South Boston, MA 02127) were prepared for photolithography with a solvent clean and adhesion promoter hexamethyldisilazane (HMDS). AZ 9260 photoresist (purchased from Integrated Micro Materials, 8141 Gateway Drive, Suite 240, Argyle, Texas 76226) was spun on the wafers and patterned to expose the channels for the devices. The etching was accomplished by utilizing deep reactive ion etching (DRIE) and the Bosch process. By alternating between sulfur hexafluoride ($[SF_6]$) as the etch gas and octafluorocyclobutane ($[C_4F_8]$) as the passivation gas, an anisotropic etch is achieved to a depth of 240μm. Excess photoresist is stripped using a combination of acetone, isopropyl alcohol, and oxygen plasma. A 10nm film of aluminum oxide ($[Al_2O_3]$) is then deposited using atomic layer deposition (ALD). Trimethylaluminum ($[Al_2(CH_3)_6]$) and water were used as precursors for this process. Afterwards, a Pyrex wafer (purchased from UniversityWafer) is anodically bonded to the silicon wafer to create an airtight seal, completing the micro-channels used as the separation column. After dicing the wafer stack, fused silica micro-capillaries (purchased from Polymicro Technologies, 18019 N25th Ave, Phoenix, AZ 85023) were connected using Miller-Stephenson Epoxy 907 (purchased from Miller-Stephenson, 6321 W. Dempster St. #302, Morton Grove, IL 60053) to complete the devices. After curing the epoxy and testing for leaks, the devices were coated with 2mg/ml of a room temperature ionic liquid: 1-butyl-3-methylimidazolium hexafluorophosphate ($[BMIm][PF_6]$) (purchased from Ionic Liquids Technologies, Inc., Tuscaloosa, AL, US) in acetone using a static coating technique [38]. The use of ionic liquids allows for very fine-tuning when it comes to applying them for a specific application. The large number of possible synthesizable ionic liquids, each with their own chemical properties and selectivity, result in a wide range of potential stationary phases [39], [40]. Moreover, there are several ionic liquid stationary phases available commercially due to the variability in their selectivity's as a stationary phase [41]. Recently, we have shown that these materials can perform as suitable stationary phases in MEMS separation columns to separate non-polar and polar compounds with robust temperature stability [36]. The columns were coated using conventional static coating techniques. The final dimensions for the device are: 1m long, 190μm wide, 240μm deep, with 20μm embedded micro-pillars. Figures 2a and 2b show optical images of these completed devices. It should be noted that the color of the channels indicates the density of the pillars in those regions as the less dense channels reflect more light than the more dense channels. Figures 2c and 2d are SEM images of the cross sections of a portion of each devices.

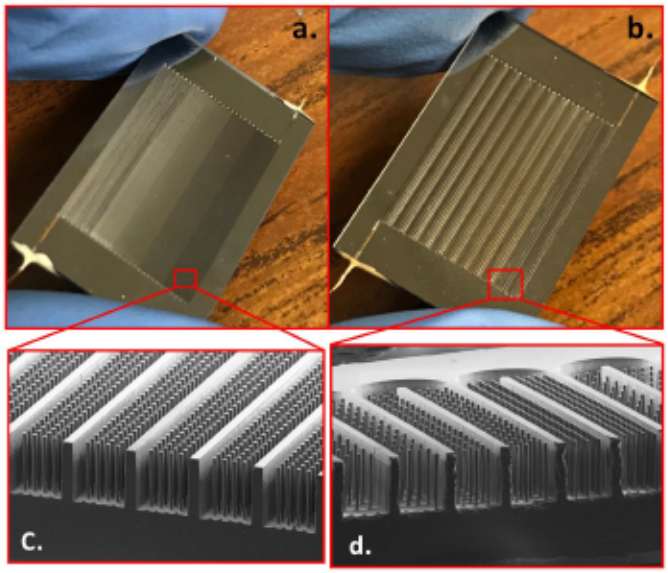

Fig. 2. (a) optical image of low density to high density geometry, (b) optical image of repeated density geometry, (c) isometric SEM image showing no change in pillar density, (d) isometric SEM image showing change in pillar density. Notice the color of the channels in the optical images as they indicate the density of that portion. Darker is more dense, lighter is less dense.

III. Experimental and Analytical Methods

A. Experimental Setup

Total volumetric flow through these devices was measured using an Agilent ADM 1000 Flowmeter at varying inlet pressures. The separation performance of these MEMS columns were evaluated using the Agilent 7890A GC-FID system. This GC system is equipped with two flame ionization detectors (FID), an automated liquid sampler (7693A) for precisely controlling injection sample size, and a conventional GC oven. For the duration of the tests, both the injector and detector were set to a temperature of 280 °C. Ultra high purity helium was used as the carrier gas for the experiments. The micro-capillary fluidic connections were fused silica capillary tubes with a total length of 30cm. Prior to testing, each device

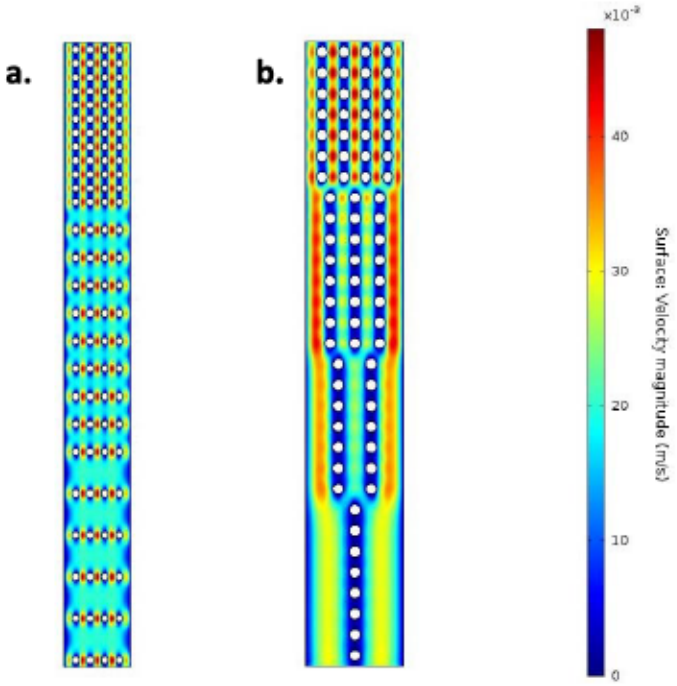

Fig. 3. COMSOL Multiphysics software fluid flow simulations for micro-pillars in a channel with: (a) varying pitch distance, (b) varying number of pillars. Notice the dark blue areas indicating close to zero velocity between the pillars as the row pitch decreases.

was conditioned in the GC system by flowing helium through it at an inlet pressure of 10 psi while the temperature of the oven was increased from 30°C to 130°C at a rate of 2°C/min.

B. Analysis Approach

Theoretical flow analysis of these columns were conducted through COMSOL Multiphysics software simulations. Figure 3 shows gas flow simulations through a channel with different micro-pillar pitch sizes. To generate these results, a pressure is applied to the bottom of the channel segments and the flow velocity is measured. As mentioned earlier, these simulation results indicate what is known as a "virtual wall." These virtual walls which can be seen in Figure 3b indicate that the pillars with a row pitch of 40μm exhibit close to zero flow between the pillars along the length of the channel. The sections with row pitches larger than 40μm show more flow between rows of pillars indicating an increase in intra-channel mixing. This mixing is not beneficial as it can lead to more peak broadening which in turn reduces the separation column efficiency. This is further corroborated by work produced from our lab as well as other groups [30], [33]. Studies performed that focus on the overall pillar density in a separation column show that as the overall pillar density increases, the separation efficiency increases as well. This is believed to be due to the effect of the embedded pillars on the effective width of the separation column which affects the height-equivalent-to-a-theoretical-plate (HETP) equation which is defined as the following:

$$HETP = A + \frac{B}{u} + C * u + D * u^2 \tag{1}$$

A is the eddy diffusion term in a packed column, B is the longitudinal diffusion term of the solute in the carrier gas, C is the resistance to mass transfer of the solute in the carrier gas and in the stationary phase, D is the extra column effects, and u is the average linear velocity of the carrier gas. As the effective width of the separation column changes, this affects the C term as the distance of mass transfer is reduced. However, it has been mentioned that semi-packed columns are not strictly controlled by this equation as the size of the pillars, the number of pillars per row as well as the pitch spacing of these rows can affect HETP [33]. As such, there is no direct correlation between the surface area inside of a semi-packed column and the separation efficiency.

For the same analyte, if a column produces more band broadening, it has less separation efficiency. This efficiency can be quantified by the number of theoretical plates (N) or the HETP. The plate number at an isothermal temperature is a function of the stationary phase material and thickness, column dimensions, the velocity of carrier gas, the carrier gas properties, the inlet and outlet pressures, and the retention factor of the analyte of interest. Columns with larger plate numbers are considered to have better separation efficiency and better separation resolution [26]. $HETP$ and N are related through the following equation:

$$HETP = \frac{L}{N} \tag{2}$$

L is the column length. For a give column geometry and shape, the column efficiency is increased as the length of the column is increased. However, this comes at the cost of increased analysis time, increased pressure requirements, and increased power requirements when performing temperature programming to separate a wide range of anlaytes in term of boiling point. In our experiments, the objective is to compare different column geometries, and hence, we chose a MEMS column length of 1m for all different designs mentioned previously. In addition, we kept the column depth as 240μm and the total column width as 190μm. We should add there are established equations that relate H to column dimensions, stationary phase, carrier gas, and operating conditions. However, these theoretical models are derived for round capillary tubings for both open-tubular and packed columns used in conventional GCs and later were expanded to include open-rectangular MEMS columns. However, there is currently no theoretical equation derived by our group or others to predict the efficiency of semi-packed columns as there are multitude of parameters that can be varied in these columns. This issue will be even more pronounced for our DMSPCs. Therefore, we used the experimental methods established in analytical chemistry to evaluate the separation efficiency of DMSPCs and control SPCs. The number of theoretical plates can be estimated by through the following equation:

$$N = 5.546 * \left(\frac{t_r}{w_h}\right)^2 \tag{3}$$

t_r is the retention time of the analyte, and w_h is the width of the peak at half of its height [42]. This equation indicates

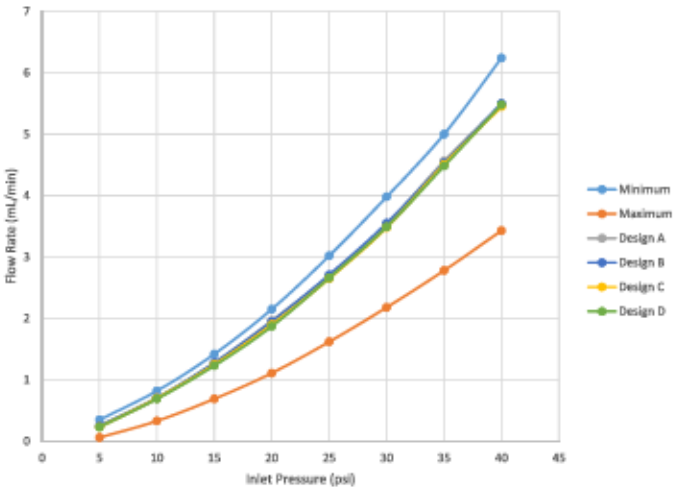

Fig. 4. Graph showing the outlet flow rate versus the inlet pressure for the different column designs measured using an Agilent ADM 1000 Flowmeter. All four of the new density modulated designs are very similar and hard to distinguish.

that a column is rewarded for retaining a peak for longer periods of time while still maintaining peak sharpness. For the purposes of this work, the plate number was calculated by using the Agilent ChemStation software bundled with the tool used. Normalization of the column efficiency with respect to its length is carried out through equation (1) and calculating H by using the measured N for each column. It is noteworthy that this method can be used if the analyte has a retention factor of 5 or more.

IV. Results and Discussion

The performance of the DMSPCs were compared against the control designs that utilized the minimum density as well as the maximum density of pillars used in the DMSPCs. It should be noted that the effect of the different topographies and geometries on column performance is the focus of this paper not the stationary phase material or the coating technique. Figure 4 shows the results of testing the volumetric flow through each design as a function of different inlet pressures. What can be seen from the graph is that the design utilizing a minimum density of pillars throughout the column provides the most total volumetric flow at any given inlet pressure. This is to be expected as it has more total volume due to a lower density of pillars than the rest of the designs. Similarly, the design with a maximum density of pillars has the lowest total flow rate at same pressure difference. Compared to these two extremes, all four DMSPC designs have very similar volumetric flow rates. Furthermore, the flow resistance of DMSPCs are closer to that of minimum control design. For instance, at 10psi, the volumetric flow rate through minimum control, DMSPCs, and maximum control are about 0.82 mL/min, 0.7 mL/min, and 0.33 mL/min, respectively. These numbers all indicate that for a given pressure the volumetric flow rate of DMSPCs is reduced only by 14% when compared to the minimum control design.

Separation efficiency was calculated by using naphthalene as the test compound at 100°C. Linear carrier gas velocity was measured by passing an un-retained methane peak and dividing the passage time by the length of the column and the micro-capillary connections. The Van Deemter plots generated from the results of these experiments can be seen in Figure 5. The average carrier gas flow velocity for the minimum control and maximum control at 10 psi pressure, for example, are 21.7 cm/s and 13.5 cm/s, respectively. For Design A, B, C, and D, the corresponding numbers are 14 cm/s, 15 cm/s, 14.2 cm/s, and 15.1 cm/s, respectively. The minimum density control shows the worst performance of the tested designs while the maximum density control shows the best overall performance when it comes to the plate numbers. These are expected as having a higher density of pillars creates a more uniform flow velocity between the rows of pillars and at the same time, minimizes the mass transfer distances [30], [32]. Figure 5a shows the separation efficiency comparison between Design A and Design B. Design A which utilizes the low-to-high density from inlet to outlet clearly produces a higher column efficiency when compared to Design B which has a density-modulation pattern that repeats itself over the length of the column. The same trend can be seen in Figure 5b when comparing the other two designs. Similar to Design B, Design D is based on the repeated arrangements of modulated pillar densities. This can be explained by looking at the generated peaks and their overall shape (not shown here). As an example, at a carrier gas flow velocity of 22cm/sec, the peak widths at half height for Designs A and B are 2.14 and 2.62 seconds, respectively, while both generating the same retention time of 22.7 seconds. The peak widths at half height for Designs C and D are 1.76 and 2.66 seconds, respectively, while both generating a retention time of 22.7 seconds, similar to Designs A and B. The peak width at half height for minimum and maximum control designs are 2.35 and 1.42 seconds, respectively. The retention times are 21.5 and 26.6 seconds for minimum and maximum control designs. This indicates that the constant repetition from a low to high density of pillars, whether through modulation of the row pitch or the number of pillars per row, over the length of the column generates more band broadening when compared to designs that use low density at the inlet and transition to high density at the outlet. This is likely due to improved uniformity of the flow through the length of the column and reduced number of intermixing of the gas. Any transition between high density to low density results in sample mixing (see Figure 3) which in turn increases band broadening. Designs B and D include more number of such transitions. The effect of intermixing in monotonic semi-packed columns have been previously investigated by our group and discussed in [27]. In summary, Design A and Design C were identified as having a better performance than Design B and Design D. On the other hand, Design C yielded a higher separation efficiency when compared to Design A as revealed by Figure 5. At 22cm/s, Design A generates a peak width at half height which is 22% greater than that of Design C. It should be mentioned again that both designs produce the same retention time of 22.7 seconds. This increase in efficiency can be attributed to a smaller row pitch spacing and the presence of virtual walls in Design C. As can be seen in Figure 3,

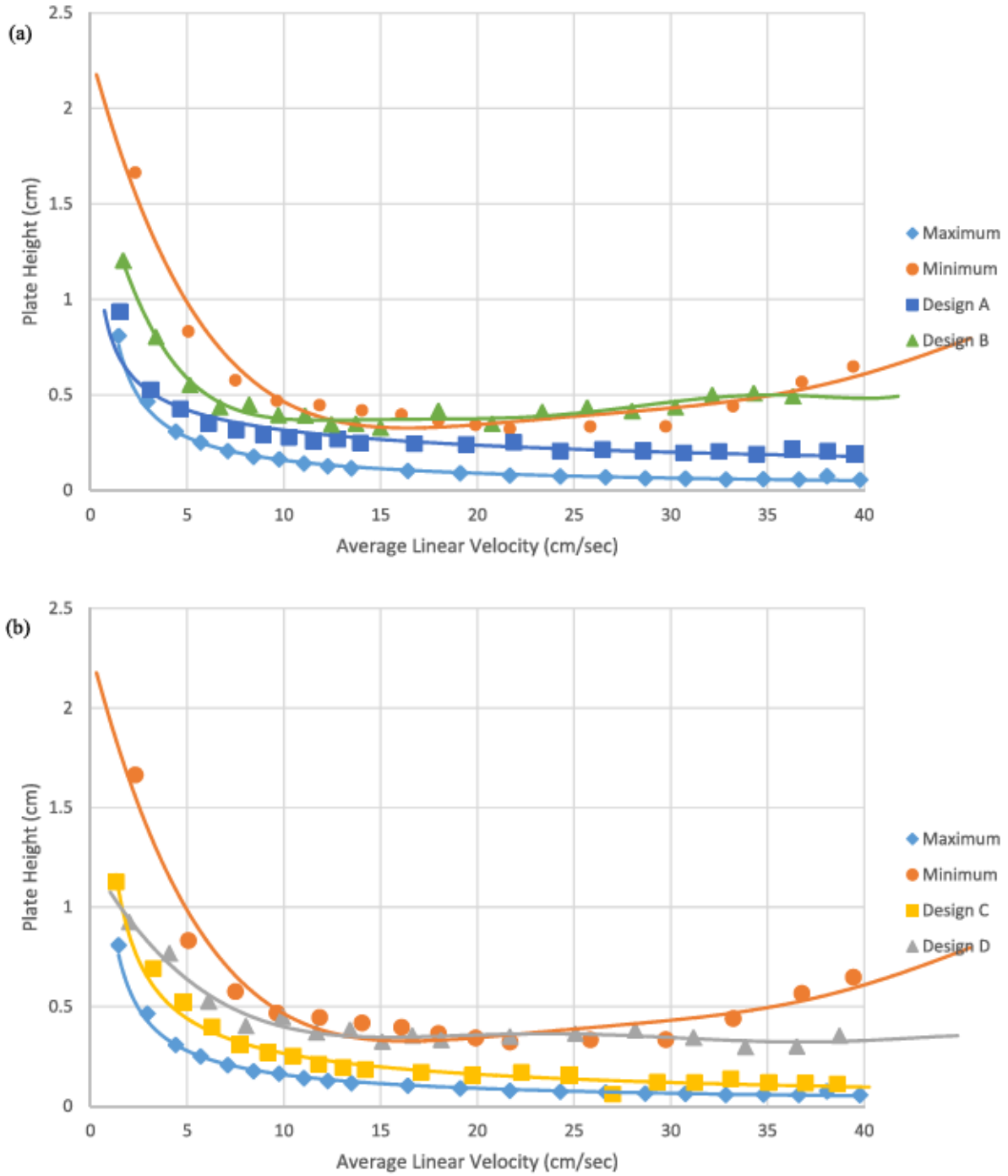

Fig. 5. Van Deemter Plot showing the height-equivalent-to-a-theoretical-plate as a function of average linear velocity for (a) Design A and Design B, (b) Design C and Design D. Chromatographic conditions: injection volume 0.1μL, split ratio 100:1, oven temperature 100°C, orientation of columns: low pillar density to high pillar density.

larger spacing between the rows in Design A increases the amount of interchannel mixing. It is notable that the data presented here show that the surface area or simply the pillar density is not the sole contributor to separation efficiency. In fact, we can see from the analysis that the pillar arrangement can have a more important role. For instance, Design A and B have the same surface area but they produce different efficiencies. This is also the case for Design C and D. Among all DMSPCs, Design C and A show better performances and both follow the same pillar arrangement. Design A produced more number of theoretical plates even though it has less number of pillars when compared to Design D.

Figure 6 shows two chromatograms generated by Design A and Design C, the two DMSPCs that exhibited the highest separation efficiency. The chromatographic conditions for these separations were: injection volume 0.1μL, split ratio of 400:1, inlet pressure of 10psi, oven temperature of 30°C for 0.15min then ramped at a rate of 40°C/min to 130°C. The compounds separated were nine n-alkanes (purchased from Sigma-Aldrich,

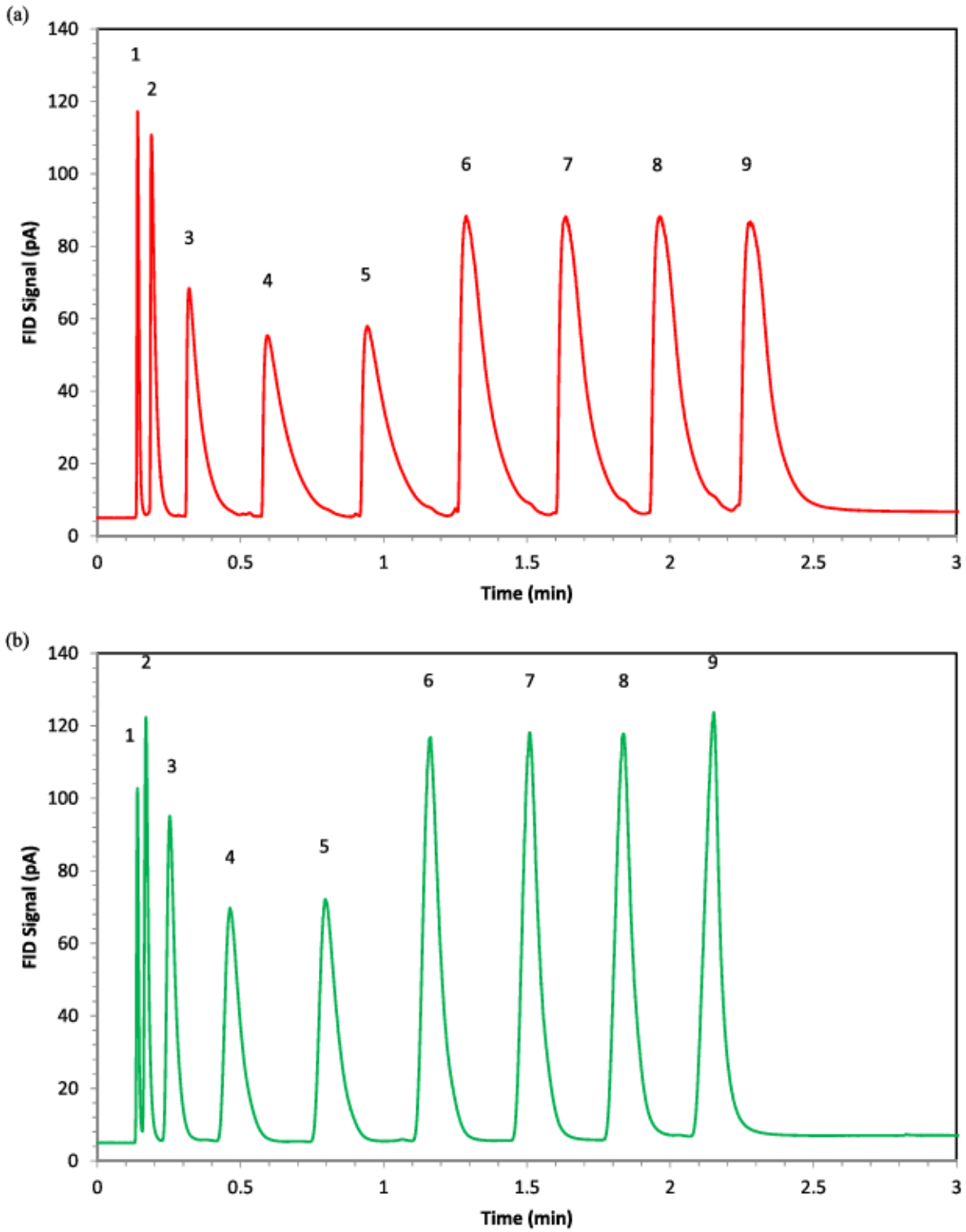

Fig. 6. Separation of a mixture containing nine n-alkanes (heptane to pentadecane). Chromatographic conditions: injection volume 0.1μl, split ratio 400:1, inlet pressure 10psi, oven temperature 30°C for 0.15 min and then ramped at the rate of 40°C/min to 130°C, orientation of the column: low pillar density to high pillar density. (a) 1st Gen ordered design, (b) 2nd Gen ordered design. Compound identification in order of elution: 1. Heptane, 2. Octane, 3. Nonane, 4. Decane, 5. Undecane, 6. Dodecane, 7. Tridecane, 8. Tetradecane, 9. Pentadecane.

3050 Spruce St., St. Louis, MO 63103) and are listed along with their boiling points in Table 2. The separation achieved by Design A shows a noticeable tailing for all the compounds while Design C creates more symmetrical peaks. All of these results indicate that Design C as a separation column exhibits volumetric flow behavior more similar to that of the minimum density design while with regards to the separation efficiency, it behaves more like the maximum density design.

We used kerosene and diesel samples to demonstrate the efficiency of our DMSPC (Design C) for the separation of

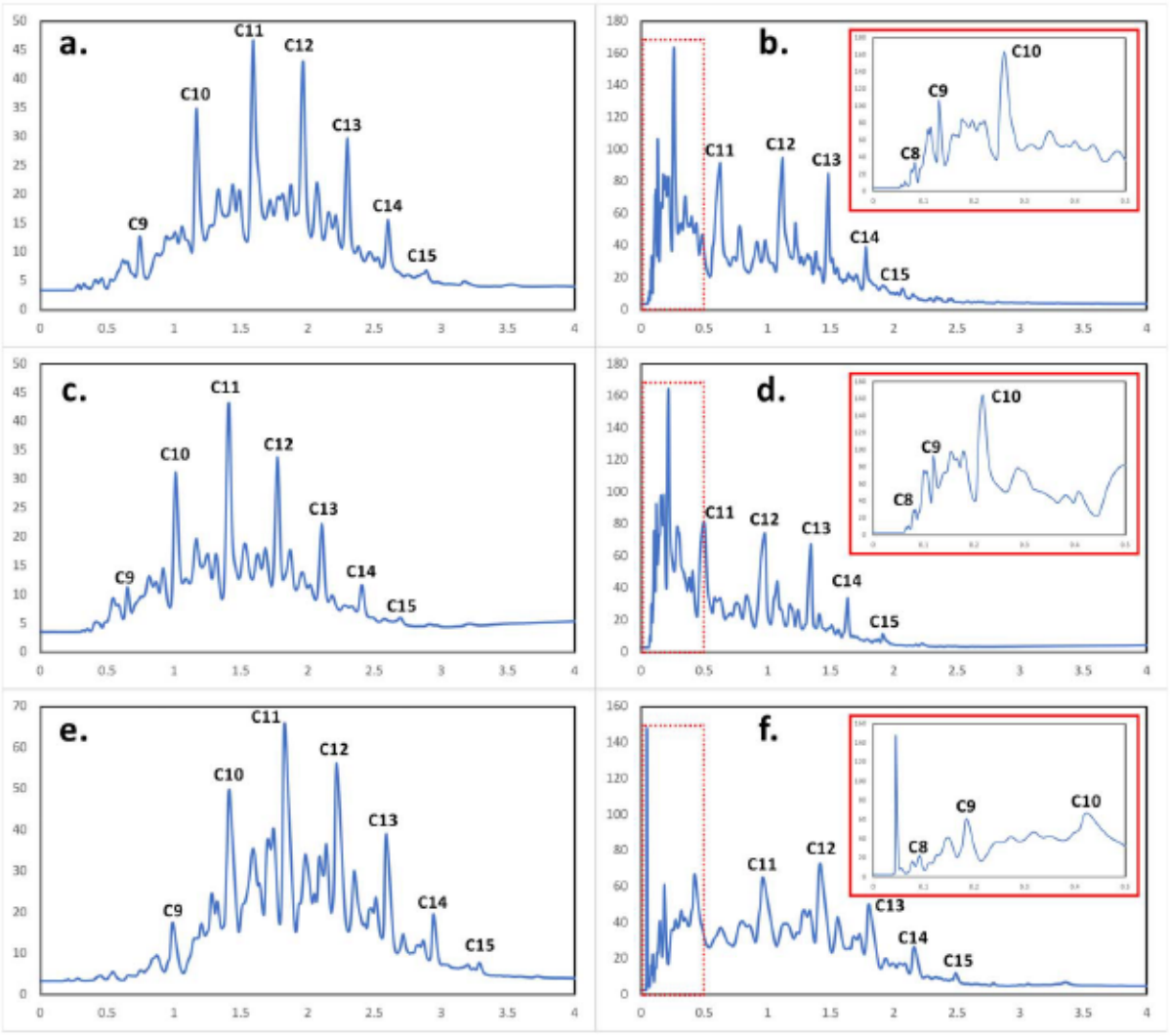

Fig. 7. Kerosene separations conducted using the maximum density design (a, b), DMSPC Design C (c, d), and minimum density design (e, f). Separations were conducted at 10psi (a, c, e) and 40psi (b, d, f). Inset from 40psi separations shows resolution differences within first half minute of chromatogram. Chromatographic conditions: injection volume 0.1μl, split ratio 400:1, oven temperature 30°C for 0.15 min and then ramped at the rate of 40°C/min to 130°C, orientation of the DMSPC column: low pillar density to high pillar density.

TABLE II
VOCs Used in Test Mixtures for GC Testing

Compounds	Boiling Point (°C)
Heptane	98
Octane	126
Nonane	151
Decane	174
Undecane	196
Dodecane	216
Tridecane	235
Tetradecane	253
Pentadecane	270

complex mixtures and compare its chromatographic performance with the control designs. Figure 7 shows a comparison of separations of kerosene at two different inlet pressures, 10psi and 40psi. The chromatographic conditions were: injection volume of 0.1μL, split ratio of 400:1, oven temperature of 30°C for 0.15min then ramped at a rate of 40°C/min to 130°C. The chromatograms generated at 10psi show the differences in the overall time required to complete the separations. It can be seen that Design C generates a faster overall separation (Figure 7c) than the maximum density design (Figure 7a). However, it does not show a significant decrease in the resolution of the major hydrocarbon constituents when compared to the maximum density design. Interestingly, the behavior shown from the minimum density design shows a separation speed that is even slower than the maximum density design. This is thought to be due to the amount of stationary phase coating deposited in the channel compared to the other two designs because static coating techniques were used. The separations conducted at an inlet pressure of 40psi further highlight the lack of resolution change between the maximum density design (Figure 7b) and Design C (Figure 7d). They also show the reduction of peak resolution in the minimum

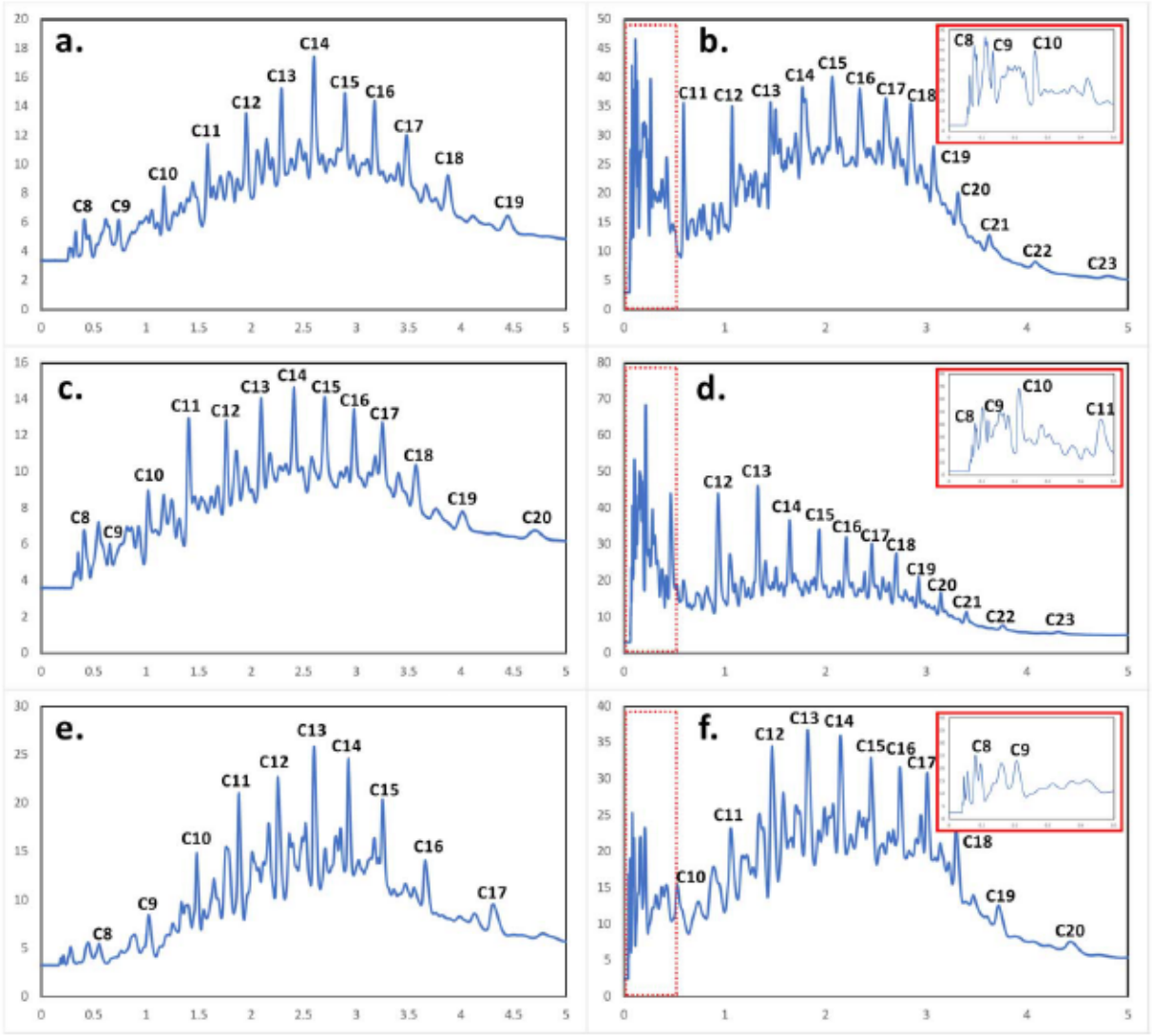

Fig. 8. Diesel separations conducted using the maximum density design (a, b), DMSPC Design C (c, d), and minimum density design (e, f). Separations were conducted at 10psi (a, c, e) and 40psi (b, d, f). Inset from 40psi separations shows resolution differences within first half minute of chromatogram. Chromatographic conditions: injection volume 0.1μl, split ratio 400:1, oven temperature 30°C for 0.15 min and then ramped at the rate of 40°C/min to 130°C, orientation of the DMSPC column: low pillar density to high pillar density.

density design (Figure 7f) at higher inlet pressures. This is better visible in the inset of the 40psi separations. It is notable that the Van Deemter curves shown in Figure 5 associated with both Design C and maximum control design show a small variation of separation efficiency with respect to the column carrier gas flow velocity (pressure) above the optimal conditions (minimum H). However, the minimum control design shows a separation efficiency more comparable to open tubular and rectangular columns as the efficiency starts to decline as the velocity is raised above the optimal flow velocity. This can explain why the separation performance of the minimum control design is more dependent on the column pressure or flow velocity. Similar chromatograms generated from separating diesel at 10psi and 40psi are shown in Figure 8. The chromatographic conditions were the same as the kerosene separations but the analysis time were limited to five minutes to show the advantages of the DMSPC. Again, it can be seen that the separation from Design C occurs faster than the maximum density design. In this case, however, an extra analyte elutes from Design C when compared to the separation from the maximum density design. Similarly to the previous separations, the chromatograms from Design C do not show any significant reduction in peak resolution of major hydrocarbons in diesel mixture compared to the maximum density design. The results shown in these two figures, which are summarized in Table 3, indicate that DMSPC can generate a faster overall separation with the same inlet pressure when compared to the maximum density SPC. However, they do not show reduced resolution or separation efficiency, behavior that is more noticeable when compared against the minimum density design. These results can also indicate that DMSPC would require a lower inlet pressure to complete the same separation in the same fixed time period when compared to the maximum density SPC. This behavior will be beneficial as it relaxes the pumping requirements needed for micro GC systems.

TABLE III

COMPARISON BETWEEN DIFFERENT DESIGNS SHOWING PILLAR DENSITY BY PERCENTAGE AREA AND MAX PLATE VALUES. TOTAL ANALYSIS TIME FOR KEROSENE SEPARATIONS IS 4 MINUTES WHILE TOTAL ANALYSIS TIME FOR DIESEL SEPARATIONS IS 5 MINUTES

	Pillar Density (%)	Max Plates	# peaks identified			
			Kerosene		Diesel	
			10psi	40psi	10psi	40psi
DMSPC Design A	5.7%	826	-	-	-	-
DMSPC Design B	5.7%	444	-	-	-	-
DMSPC Design C	12.7%	2568	38	54	52	78
DMSPC Design D	12.7%	472	-	-	-	-
Maximum Control	14.7%	2732	45	65	54	83
Minimum Control	1.3%	449	39	44	49	59

V. CONCLUSION

In this work, we successfully developed new semi-packed MEMS separation columns utilizing pillar density modulation to increase total volumetric flow compared to monotonic SPCs having a highly packed pillar arrays. The density modulated column provided separation efficiencies which were superior over the monotonic minimum density (low packed) SPC and were more similar to that of maximum density SPCs. Two methods for modulating pillar density were developed and arranged in two different ways resulting in four unique DMSPC topographies. These were then compared with two control designs utilizing a minimum density of pillars and a maximum density of pillars. Of these four, Design C was shown to perform the best with regards to separation efficiency. This DMSPC performed separations on kerosene and diesel that were faster than the maximum density design under the same chromatographic conditions without any significant loss of peak resolution. This indicates that DMSPC could be used in micro GC systems for reducing the pressure requirements or in near-real-time analysis systems to reduce the time necessary for a separation to complete. Based on the experimental data, DMSPC might show an even larger advantage as the length of the separation columns increases for separation of a wider range of analytes and in more complex environments. This new column design introduces a new alternative when it comes to choosing a high performance separation column with lower pressure requirements for the use in a micro GC system.

ACKNOWLEDGMENT

The work was conducted primarily by the support of the National Science Foundation under award number ECCS 1711699. The authors would like to acknowledge Ms. Ana Lopez for her help in conducting the COMSOL Multiphysics simulation work. The fabrication of the MEMS chips were performed at Virginia Tech Micro/Nano Fabrication Facilities. SEM imaging were done at Virginia Tech Nano Characterization and Fabrication Laboratory (NCFL).

REFERENCES

[1] R. Chan, A. Lopez, B. P. Regmi, and M. Agah, "Micro-pillar density modulation in semi-packed MEMS column," in *Proc. 19th Int. Conf. Solid-State Sens., Actuators Microsyst. (TRANSDUCERS)*, Jun. 2017, pp. 1528–1531.

[2] M. Zhou, J. Lee, H. Zhu, R. Nidetz, K. Kurabayashi, and X. Fan, "A fully automated portable gas chromatography system for sensitive and rapid quantification of volatile organic compounds in water," *RSC Adv.*, vol. 6, no. 55, pp. 49416–49424, 2016.

[3] M. Akbar, M. Restaino, and M. Agah, "Chip-scale gas chromatography: From injection through detection," *Microsyst. Nanoeng.*, vol. 1, Dec. 2015, Art. no. 15039.

[4] J. H. Sun, D. F. Cui, X. Chen, L. L. Zhang, H. Y. Cai, and H. Li, "A micro gas chromatography column with a micro thermal conductivity detector for volatile organic compound analysis," *Rev. Sci. Instrum.*, vol. 84, no. 2, p. 025001, Jan. 2013.

[5] W. R. Collin, A. Bondy, D. Paul, K. Kurabayashi, and E. T. Zellers, "μGC $\times$ μGC: Comprehensive two-dimensional gas chromatographic separations with microfabricated components," *Anal. Chem.*, vol. 87, no. 3, pp. 1630–1637, Feb. 2015.
[6] H. Kim *et al.*, "A micropump-driven high-speed MEMS gas chromatography system," in *Proc. Int. Solid-State Sens., Actuators Microsyst. Conf. (TRANSDUCERS)*, Jun. 2007, pp. 1505–1508.
[7] C.-J. Lu *et al.*, "First-generation hybrid MEMS gas chromatograph," *Lab Chip*, vol. 5, no. 10, pp. 1123–1131, 2004.
[8] S. K. Kim, H. Chang, and E. T. Zellers, "Microfabricated gas chromatograph for the selective determination of trichloroethylene vapor at sub-parts-per-billion concentrations in complex mixtures," *Anal. Chem.*, vol. 83, no. 18, pp. 7198–7206, Sep. 2011.
[9] E. T. Zellers *et al.*, "An integrated micro-analytical system for complex vapor mixtures," in *Proc. Int. Solid-State Sens., Actuators Microsyst. Conf. (TRANSDUCERS)*, Jun. 2007, pp. 1491–1496.
[10] J. Wang *et al.*, "Compact prototype microfabricated gas chromatographic analyzer for autonomous determinations of VOC mixtures at typical workplace concentrations," *Microsyst. Nanoeng.*, vol. 4, Apr. 2018, Art. no. 17101.
[11] T.-H. Tzeng *et al.*, "A portable micro gas chromatography system for lung cancer associated volatile organic compound detection," *IEEE J. Solid-State Circuits*, vol. 51, no. 1, pp. 259–272, Jan. 2016.
[12] H. Shakeel, D. Wang, J. R. Heflin, and M. Agah, "Width-modulated microfluidic columns for gas separations," *IEEE Sensors J.*, vol. 14, no. 10, pp. 3352–3357, Oct. 2014.
[13] H. Yuan *et al.*, "The effect of the channel curve on the performance of micromachined gas chromatography column," *Sens. Actuators B, Chem.*, vol. 239, pp. 304–310, Feb. 2017.
[14] H. Yuan, X. Du, Y. Li, and Y. Jiang, "Mems-based semi-packed gas chromatography column with wavy channel configuration," in *Proc. IEEE Int. Conf. Manipulation, Manuf. Meas. Nanosc. (3M-NANO)*, Jul. 2016, pp. 283–286.
[15] D. W. Armstrong, L. He, and Y. S. Liu, "Examination of ionic liquids and their interaction with molecules, when used as stationary phases in gas chromatography," *Anal. Chem.*, vol. 71, no. 17, pp. 3873–3876, Sep. 1999.
[16] L. Li, M. Wu, Y. Feng, F. Zhao, and B. Zeng, "Doping of three-dimensional porous carbon nanotube-graphene-ionic liquid composite into polyaniline for the headspace solid-phase microextraction and gas chromatography determination of alcohols," *Analytica Chim. Acta*, vol. 948, pp. 48–54, Dec. 2016.
[17] G. Serrano, S. M. Reidy, and E. T. Zellers, "Assessing the reliability of wall-coated microfabricated gas chromatographic separation columns," *Sens. Actuators B, Chem.*, vol. 141, no. 1, pp. 217–226, Aug. 2009.
[18] I. Azzouz *et al.*, "Review of stationary phases for microelectromechanical systems in gas chromatography: Feasibility and separations," *Anal. Bioanal. Chem.*, vol. 406, no. 4, pp. 981–994, Feb. 2014.
[19] J. Vial *et al.*, "Silica sputtering as a novel collective stationary phase deposition for microelectromechanical system gas chromatography column: Feasibility and first separations," *J. Chromatography A*, vol. 1218, no. 21, pp. 3262–3266, May 2011.
[20] S. C. Terry, J. H. Jerman, and J. B. Angell, "A gas chromatographic air analyzer fabricated on a silicon wafer," *IEEE Trans. Electron Devices*, vol. 26, no. 12, pp. 1880–1886, Dec. 1979.
[21] M. Agah, G. R. Lambertus, R. D. Sacks, and K. D. Wise, "High-speed MEMS-based gas chromatography," in *IEDM Tech. Dig.*, Dec. 2004, pp. 27–30.
[22] J. A. Potkay, J. A. Driscoll, M. Agah, R. D. Sacks, and K. D. Wise, "A high-performance microfabricated gas chromatography column," in *Proc. IEEE 16th Annu. Int. Conf. Micro Electro Mech. Syst. (MEMS)* Kyoto, Japan, Jan. 2003, pp. 395–398.
[23] M. J. D. Boer *et al.*, "Micromachining of buried micro channels in silicon," *J. Microelectromech. Syst.*, vol. 9, no. 1, pp. 94–103, Mar. 2000.
[24] G. Lambertus *et al.*, "Design, fabrication, and evaluation of microfabricated columns for gas chromatography," *Anal. Chem.*, vol. 76, no. 9, pp. 2629–2637, May 2004.
[25] M. A. Zareian-Jahromi, M. Ashraf-Khorassani, L. T. Taylor, and M. Agah, "Design, modeling, and fabrication of MEMS-based multicapillary gas chromatographic columns," *J. Microelectromech. Syst.*, vol. 18, no. 1, pp. 28–37, Feb. 2009.
[26] H. M. McNair and E. J. Bonelli, *Basic Gas Chromatography*, vol. 150. Walnut Creek, CA, USA: Varian Aerograph, 1969.
[27] S. Ali, M. Ashraf-Khorassani, L. T. Taylor, and M. Agah, "MEMS-based semi-packed gas chromatography columns," *Sens. Actuators B, Chem.*, vol. 141, no. 1, pp. 309–315, Aug. 2009.
[28] Y. Li *et al.*, "Improvement of column efficiency in MEMS-Based gas chromatography column," *RSC Adv.*, vol. 4, no. 8, pp. 3742–3747, 2014.
[29] B. Tian *et al.*, "Research on micro-fabricated gas chromatographic columns with embedded ellipitic cylindrical posts," in *Proc. IEEE 30th Int. Conf. Micro Electro Mech. Syst. (MEMS)*, Jan. 2017, pp. 1343–1346.
[30] S. Nishiyama, T. Nakai, M. Shuzo, J.-J. Delaunay, and I. Yamada, "Effect of micropillar density on separation efficiency of semi-packed micro gas chromatographic columns," in *Proc. IEEE SENSORS*, Oct. 2009, pp. 1935–1938.
[31] H. Shakeel and M. Agah, "High density semipacked separation columns with optimized atomic layer deposited phases," *Sens. Actuators B, Chem.*, vol. 242, pp. 215–223, Apr. 2017.
[32] B. Alfeeli, S. Narayanan, M. McMillan, D. Hirtenstein, G. Rice, and M. Agah, "The effect of pillar array in semi-packed micro gas chromatography," in *Proc. IEEE SENSORS*, Oct. 2011, pp. 1097–1100.
[33] B. Alfeeli *et al.*, "Interchannel mixing minimization in semi-packed micro gas chromatography columns," *IEEE Sensors J.*, vol. 13, no. 11, pp. 4312–4319, Nov. 2013.
[34] A. D. Radadia, A. Salehi-Khojin, R. I. Masel, and M. A. Shannon, "The effect of microcolumn geometry on the performance of micro-gas chromatography columns for chip scale gas analyzers," *Sens. Actuators B, Chem.*, vol. 150, no. 1, pp. 456–464, Sep. 2010.
[35] H. Purnell, *Gas Chromatography*. Hoboken, NJ, USA: Wiley, 1967.
[36] B. P. Regmi, R. Chan, and M. Agah, "Ionic liquid functionalization of semi-packed columns for high-performance gas chromatographic separations," *J. Chromatography A*, vol. 1510, pp. 66–72, Aug. 2017.
[37] H. Shakeel, G. W. Rice, and M. Agah, "Semipacked columns with atomic layer-deposited alumina as a stationary phase," *Sens. Actuators B, Chem.*, vol. 203, pp. 641–646, Nov. 2014.
[38] G. Rutten and J. A. Rijks, "Technique for static coating of glass capillary columns," *J. High Resolution Chromatography*, vol. 1, no. 5, pp. 279–280, 1978.
[39] M. Deetlefs and K. R. Seddon, "Ionic liquids: Fact and fiction," *Chim. Oggi-Chem. Today*, vol. 24, no. 2, p. 16, 2006.
[40] R. D. Rogers, "Reflections on ionic liquids," *Nature*, vol. 447, no. 7147, pp. 917–918, Jun. 2007.
[41] C. F. Poole and S. K. Poole, "Ionic liquid stationary phases for gas chromatography," *J. Separat. Sci.*, vol. 34, no. 8, pp. 888–900, Apr. 2011.
[42] A. D. Radadia, R. D. Morgan, R. I. Masel, and M. A. Shannon, "Partially buried microcolumns for micro gas analyzers," *Anal. Chem.*, vol. 81, no. 9, pp. 3471–3477, May 2009.

Authors' photographs and biographies not available at the time of publication.